

Supporting Information

Highly responsive UV-photodetectors based on single electrospun TiO₂ nanofibres

Aday J. Molina-Mendoza,^a Alicia Moya,^b Riccardo Frisenda,^c Simon A. Svatek,^c Patricia Gant,^c Sergio Gonzalez-Abad,^c Elisa Antolin,^d Nicolás Agraït,^{a,c,e} Gabino Rubio-Bollinger,^{a,e} David Perez de Lara,^c Juan J. Vilatela,^b and Andres Castellanos-Gomez.^c

- ^{a.} *Departamento de Física de la Materia Condensada, Universidad Autónoma de Madrid, Campus de Cantoblanco, E-28049, Madrid, Spain. E-mail: aday.molina@uam.es*
- ^{b.} *IMDEA materials institute, Eric Kandel 2, Getafe, Madrid, 28906 Spain. E-mail: juanjose.vilatela@imdea.org*
- ^{c.} *Instituto Madrileño de Estudios Avanzados en Nanociencia (IMDEA-nanociencia), Campus de Cantoblanco, E-28049 Madrid, Spain. E-mail: andres.castellanos@imdea.org*
- ^{d.} *Instituto de Energía Solar – Universidad Politécnica de Madrid ETSI Telecomunicación, Ciudad Universitaria sn, 28040 Madrid, Spain.*
- ^{e.} *Condensed Matter Physics Center (IFIMAC), Universidad Autónoma de Madrid, E-28049 Madrid, Spain.*

In this supporting information we include the following content:

- Electrospun TiO₂ nanofibre synthesis
- Photodetector fabrication method
- More photodetectors characterization
- Photodetectors based on TiO₂ nanofibres annealed in air
- Photodetectors performance under different atmospheres

Electrospun TiO₂ nanofibre synthesis

In this work, we use a sol-gel based electrospinning method to produce TiO₂ nanofibres. A polymer solution of PVP (polyvinylpyrrolidone, 10%wt.) in ethanol is mixed with an alcoholic solution of metal precursor (titanium ethoxide, 63%wt.) and acetic acid as catalyst of the sol-gel reaction. After reaching a homogeneous solution, it is loaded into a syringe placed in the electrospinning set-up (Nanon 01A, MECC CO., LTD.). A continuous mesh of fibres is collected at 10 cm distance from the tip and using an applied voltage of 18 kV and 2 mL/h of flow rate. After electrospinning, the fibres are thermally treated in air to remove the polymer at 400 °C for 2.5 hours and then annealed in Ar at 500 °C for 1 hour to complete the crystallisation of the metal oxide. In addition, a sample of TiO₂ fibre annealed in air at 500°C for 1 hour was also prepared and used for a preliminary evaluation of the effect of the annealing atmosphere on the photoconduction mechanism and properties of devices.

The nanofibre structure consists of a mesoporous network of well-ordered TiO₂ nanocrystals and presents two main features different from standard TiO₂ produced by sol-gel, namely, 1) the use of the polymer keep the titanium sol unit which accelerates the crystallisation and the anatase-to-rutile phase transformation, creating tight interfaces between the TiO₂ nanocrystals and 2) the annealing in inert atmosphere produces oxygen vacancies.¹⁻³ Both phenomena, interfaces and vacancies, facilitate the creation of internal junction with new electronic states that could trap electrons and ultimately increase lifetime and diffusion coefficients of charge carriers in the material.

Photodetector fabrication method

In Fig. S1 **1** to **4** we can see in the pictures, through the PDMS stamp, the pre-patterned Au electrodes on a SiO₂ substrate and some blurred shapes. These blurred shapes are the TiO₂ nanofibres after been peeled off from the thin film, as seen from the backside of the stamp, out of focus. When the stamp is approaching the surface, the flakes get more and more focused and we can align substrate and sample (picture **3**). Finally, when the stamp gets in contact with the substrate, we see a change in the color of both the substrate and the flake (picture **4**). In Fig. S1 **5** to **9** we show pictures of the PDMS been peeled off from the substrate in order to transfer the nanofibers. It is possible to recognize the part of the PDMS which is already peeled off from the one that is still in contact with the substrate by the difference in the color. The line that moves from one picture to the next one is the meniscus that separates the peeled stamp from the part still in contact. Once the meniscus has passed the flake, we can completely remove the stamp.

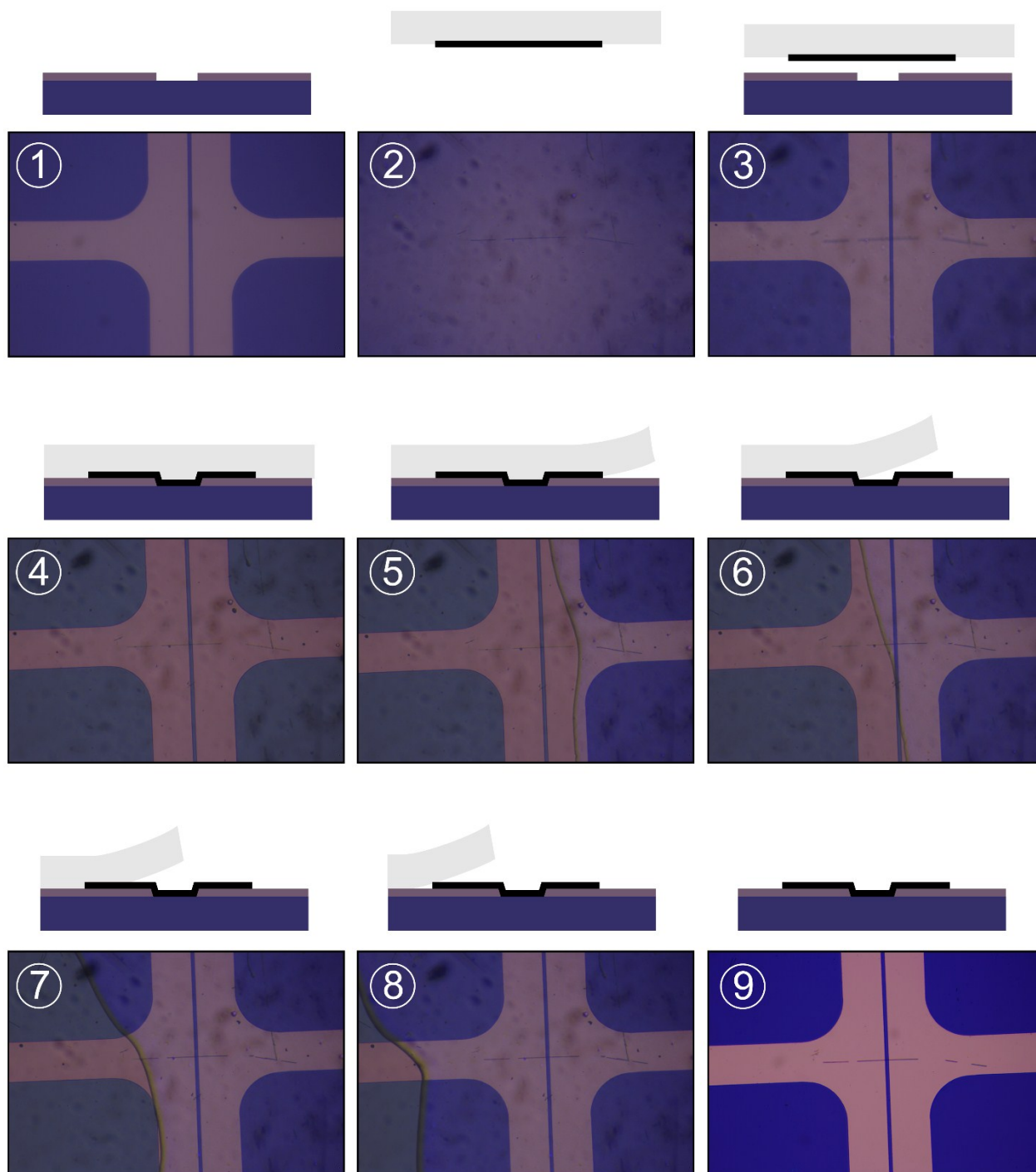


Fig. S1. Optical microscopy images of the fabrication of a TiO_2 nanofibre-based photodetector. From 1 to 4: the PDMS stamp is approached to the substrate and the nanofiber is aligned to the electrodes. From 5 to 9: the PMDS stamp is slowly peeled off to transfer the nanofibre.

More photodetectors characterization

Photodetector 1

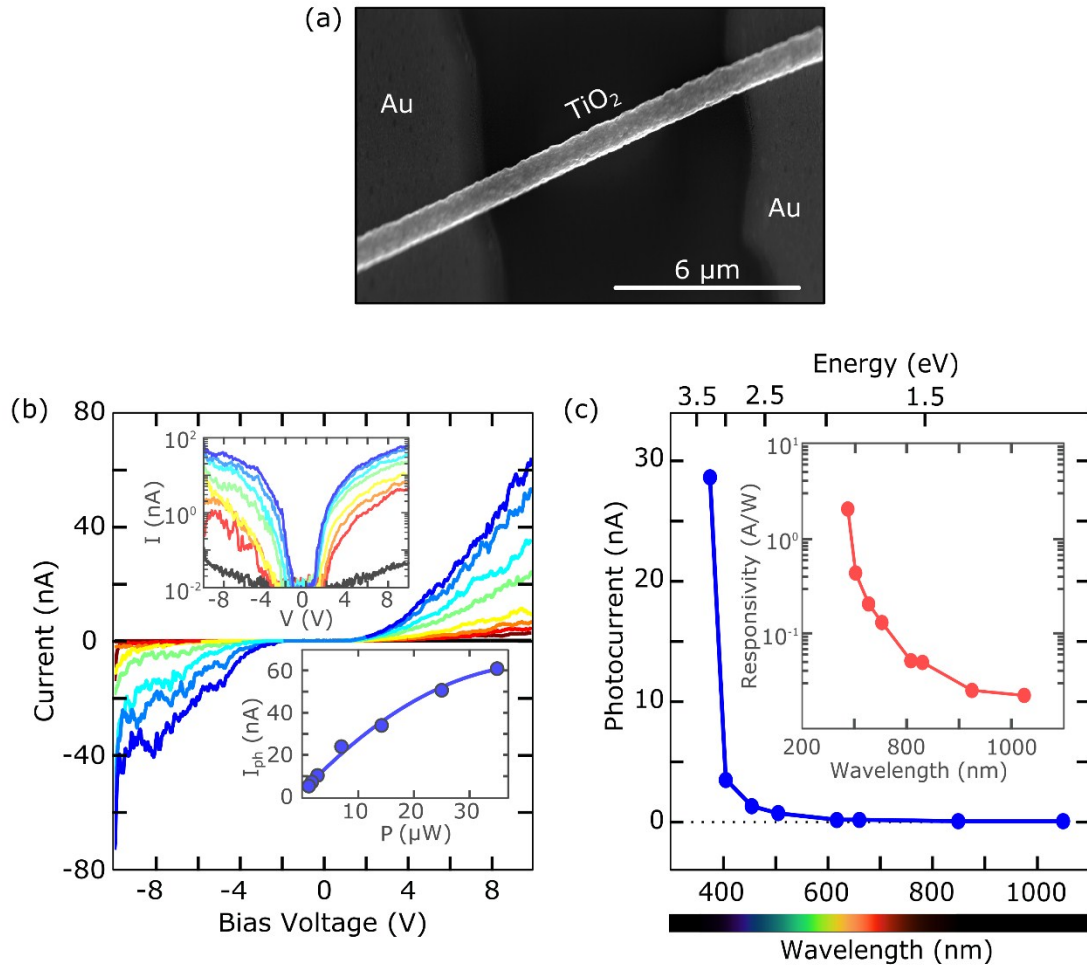


Fig. S2 (a) SEM image of a TiO₂ photodetector. (b) Current-voltage characteristics upon illumination with light wavelength 375 nm excitation for increasing light powers up to 35 μW. Upper inset shows the current-voltage characteristics in a semilogarithmic plot. Lower inset shows photocurrent for increasing powers. The solid line is a power law fit. (c) Photocurrent measured as a function of different laser wavelengths ($P = 15 \mu\text{W}$). Measurements are taken at $V_{ds} = 10 \text{ V}$. Inset shows a semilogarithmic plot of the responsivity as a function of the wavelength. Solid lines are guides.

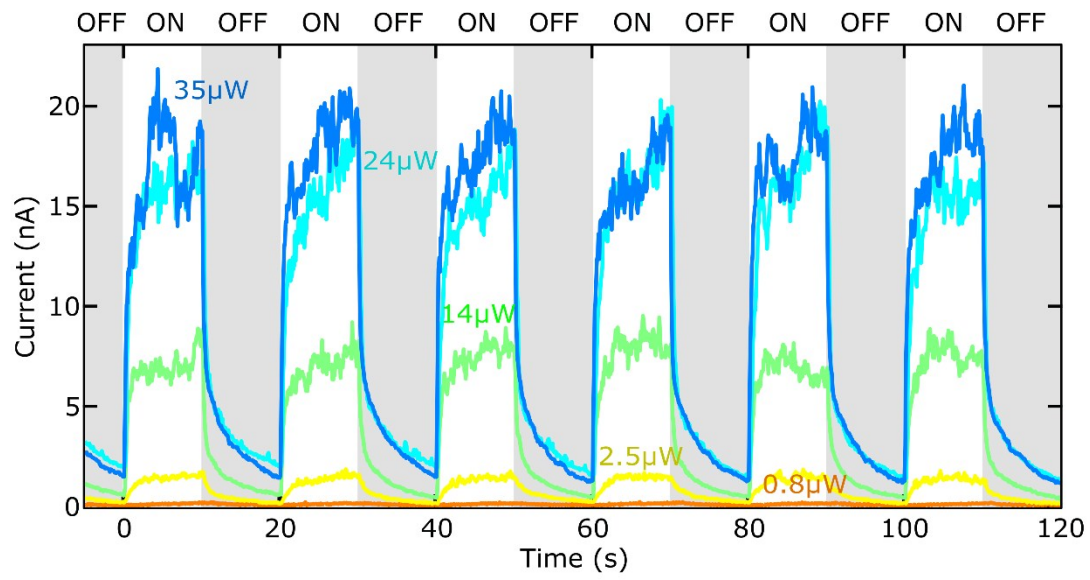


Fig. S3 Current time response of the device shown in Fig. S2 under a 100 mHz modulated optical excitation ($\lambda = 375\text{nm}$) for increasing laser powers up to $35\text{ }\mu\text{W}$. Measurements are acquired at $V_b = 10\text{ V}$.

Photodetector 2

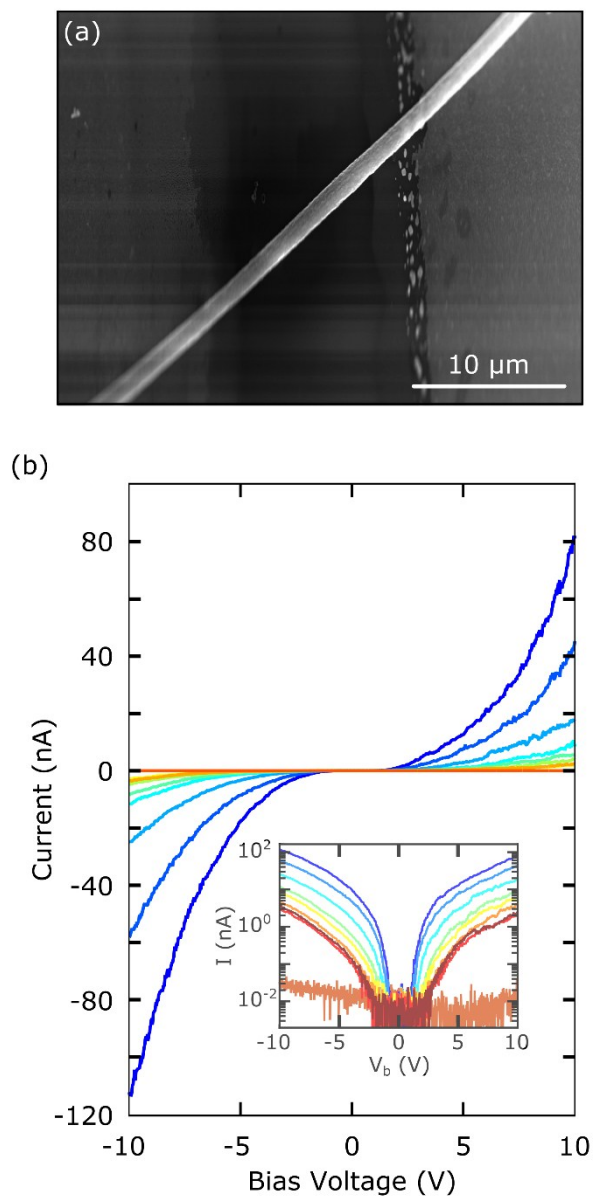


Fig. S4 (a) SEM image of a TiO_2 photodetector. **(b)** Current-voltage characteristics upon illumination with light wavelength 405 nm excitation for increasing light powers up to $250\ \mu\text{W}$. The inset shows the current-voltage characteristics in a semilogarithmic plot.

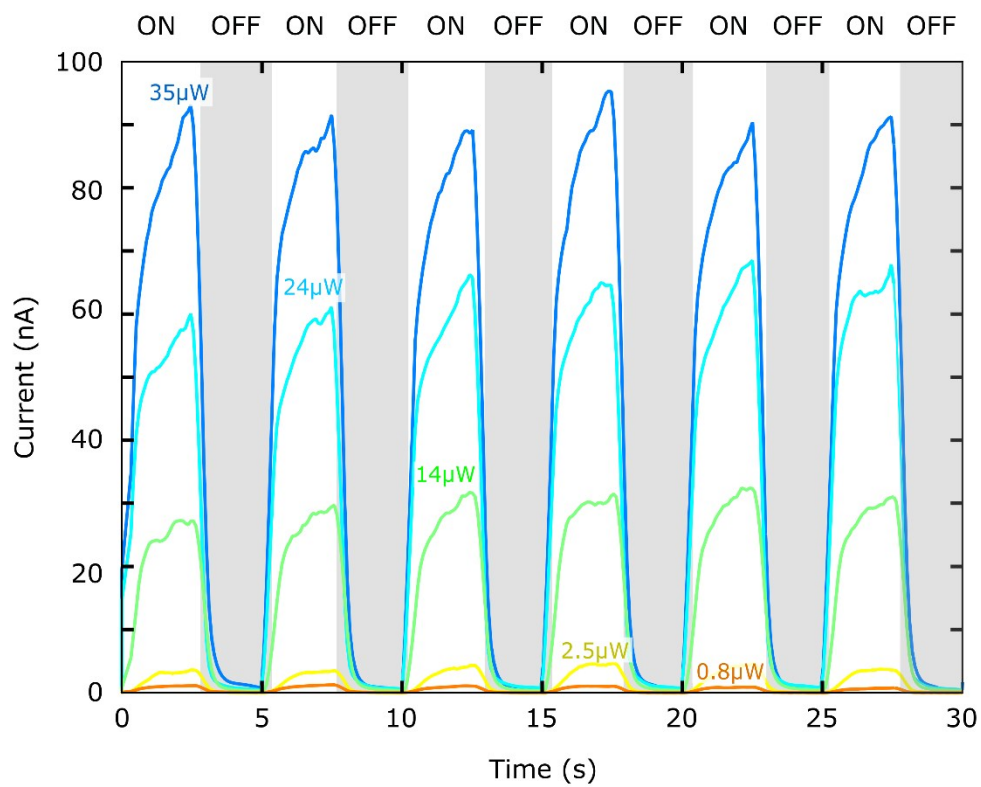


Fig. S5 Time response of the device shown in Fig. S4 upon a 500 MHz modulated optical excitation ($\lambda = 375\text{ nm}$) for increasing laser powers up to 35 μW . Measurements are taken at $V_b = 10\text{ V}$.

Photodetectors based on TiO₂ nanofibres annealed in air

We have investigated the role played by the crystallisation atmosphere in the performance of TiO₂ nanofibres-based photodetectors. The nanofibre characterized in Fig. S6 and S7 has been synthesized following exactly the same synthetic procedure than the TiO₂ fibres from the main text except that it was crystallised in air. The electronic characterization of the device in air (not shown) yields low conductivity with current values lower than 1 pA for $V_b = 10$ V. We first study the response to incident light of the photodetector by calculating the responsivity as function of the light power ($\lambda = 375$ nm, $V_b = 10$ V, Fig. S6), which reaches a maximum value of ~ 33 A/W.

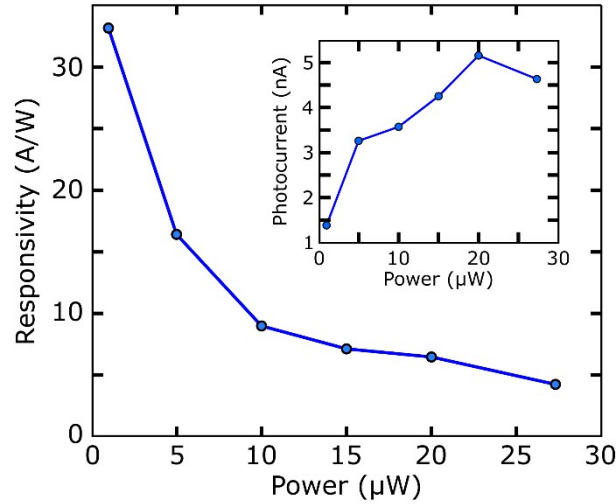


Fig. S6 Responsivity as a function of the light power of the photodetector based on a single TiO₂ nanofibre annealed in air. The maximum value achieved is of 33 A/W. Inset: photocurrent generated in the photodetector as a function of the light power.

We also study the responsivity of the device as a function of the light wavelength, shown in Fig. S7. It is important to note here that the photoresponse as a function of the light wavelength has been measured for the maximum power provided by the LED sources for each wavelength, since the response to lower incident light powers for light wavelengths larger than 405 nm were too small to be measured with our experimental setup. The highest responsivity (~ 4 A/W) in this case is obtained for a light wavelength of $\lambda = 375$ nm ($V_b = 10$ V).

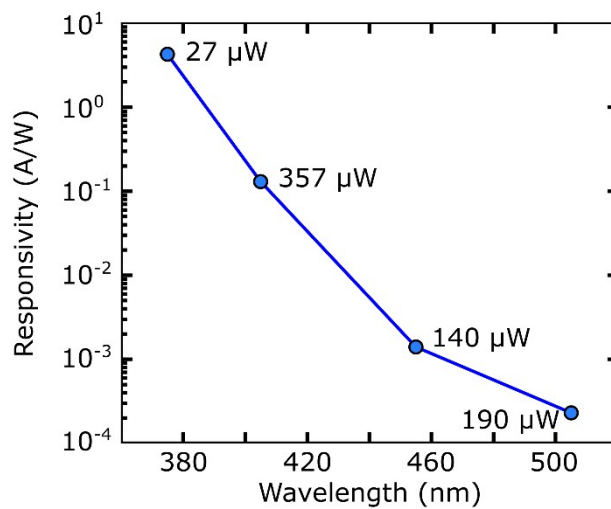


Fig. S7 Responsivity as a function of the light wavelength of the photodetector based on a single TiO₂ nanofibre annealed in air. The maximum value (~ 4 A/W) is obtained for a light wavelength of $\lambda = 375$ nm ($V_b = 10$ V).

Photodetectors performance under different atmospheres

The photoresponse of two more devices apart from the one shown in the main text (Fig. 4) have been measured under different atmosphere. The dark current of the devices in vacuum (10^{-5} mbar) and in oxygen atmosphere (1 bar), where it is possible to see that the dark current is enhanced in vacuum with respect to oxygen (Fig. S8a). Another device has been measured in vacuum (10^{-5} mbar) and in air (Fig. S8b), showing a higher dark current in vacuum than in air, giving evidence that the oxygen adsorbed on the nanofibre surface might be playing a role in the conductance in the material.

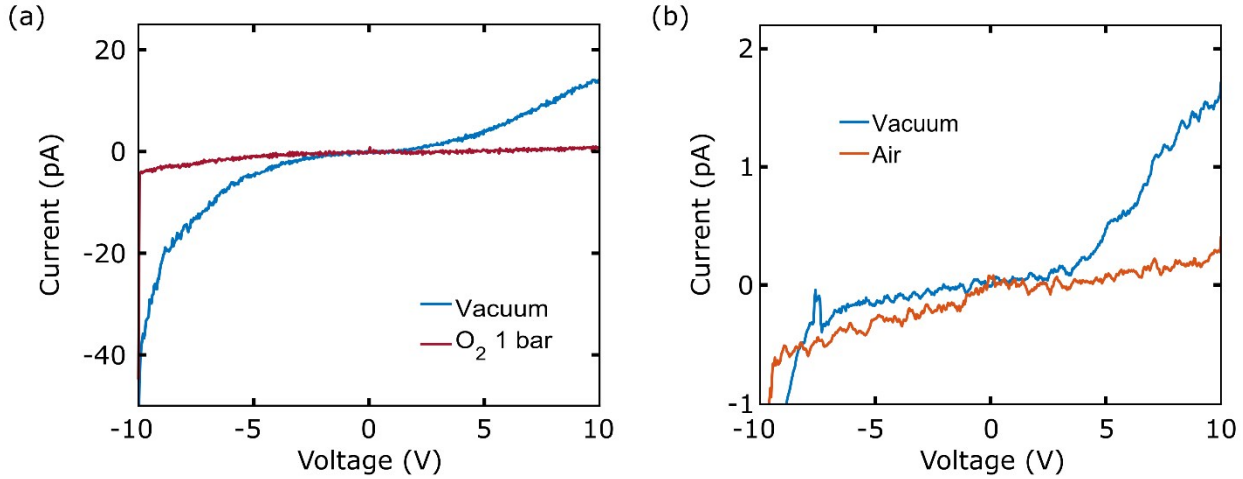


Fig. S8 (a) Current-voltage characteristic in dark conditions of a device in vacuum (10^{-5} mbar) and in oxygen (1 bar). The dark current in oxygen is lower than in vacuum. **(b)** Current-voltage characteristic in dark conditions of a device in vacuum (10^{-5} mbar) and in air. The dark current in air is lower than in vacuum.

We have also measured the photoresponse (wavelength of 455 nm, light intensity 0.7 W/cm^2) of the devices shown in Fig. S6 as a function of time. The time response in vacuum (10^{-5} mbar) is considerably slower than in oxygen (Fig. S9a) and in air (Fig. S9b), especially regarding the fall time. In Fig. S9a, the fall time of the device in vacuum is >100 s, while in oxygen is ~ 80 s. In Fig. S9b, the fall time of the device in vacuum is ~ 90 s, while in air it is <1 s, suggesting that the adsorbed oxygen and the water molecules on the fibre surface are playing an important role in the time response of the material.

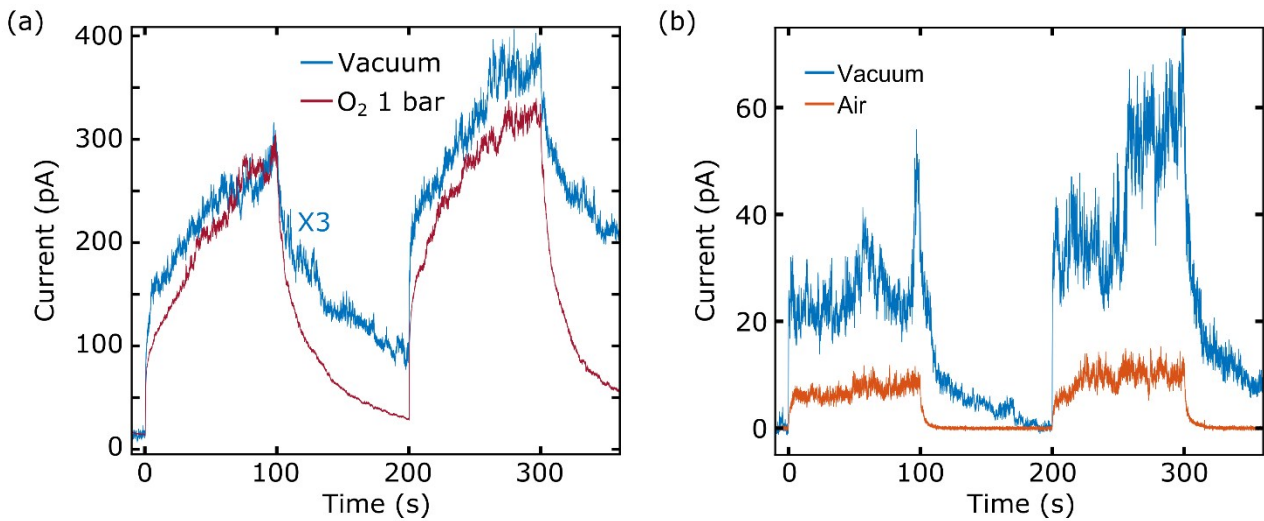


Fig. S9 (a) Photoresponse of a device as a function of time in vacuum (10^{-5} mbar) and in oxygen (1 bar). The fall time is considerably slower in vacuum (>100 s) than in oxygen (~ 90 s). **(b)** Photoresponse of another device as a function of time in vacuum (10^{-5} mbar) and in air. The fall time is considerably slower in vacuum (~ 80 s) than in air (~ 1 s).

Supporting Information references

- [1] A. Moya, A. Cherevan, S. Marchesan, P. Gebhardt, M. Prato, D. Eder and J. J. Vilatela, *Applied Catalysis B: Environmental*, 2015, **179**, 574-582
- [2] J.M.G. Amores, V.S. Escribano, G. Busca, *J. Mater. Chem.*, 1995, **5**, 1245.
- [3] H. Zhang, J. Banfield, *Am. Miner.*, 1999, **84**, 528–535.